RESEARCH ARTICLE

A 90-year record of glacier changes in the Novaya Zemlya Archipelago, Russian High Arctic

Dean R. Maraldo & Woonsup Choi
Department of Geography, University of Wisconsin-Milwaukee, Milwaukee, WI, USA

Abstract

Glacial retreat in the Russian High Arctic, particularly in the Novaya Zemlya Archipelago (NZA), is emblematic of global warming. Some global models project that, by 2100, sea-level rise contributions from melting glaciers in this region could be comparable to contributions from Antarctica's and Greenland's peripheral glaciers. However, historical glacier change in the NZA remains poorly known. Here, we present the longest decadal chronology of glacier change in the NZA to date, including a 90-year record (ca. 1931–2021) of frontal length change, and a 70-year record (1952–2021) of glacier area change. Using a combination of survey records, historical maps and satellite imagery, we analyse changes for 63 outlet glaciers, representing 86% of the NZA's total ice mass. Our results show that the average frontal retreat rate increased each decade since the early 1970s, reaching a peak retreat rate of 65 m a^{-1} between 2011 and 2021. Glaciers terminating in the Barents Sea experienced the greatest losses, retreating an average of 4.2 km (11.6%) since 1952. During this time, the total glacier area decreased by 1606 km^2 (10%). We identified increasing summer air and sea-surface temperatures as key drivers of accelerated glacier retreat, with peak air and sea-surface temperatures occurring from 2011 to 2021, corresponding to the period with the fastest retreat rates and the largest glacier area loss.

Keywords

Climate change; glacier retreat; satellite imagery; sea-surface temperature

Correspondence

Dean R. Maraldo, Department of Geography, University of Wisconsin-Milwaukee, P.O. Box 413, Bolton Hall, Milwaukee, WI, 53201, USA.
E-mail: dmaraldo@uwm.edu

Abbreviations

ERSSTv5: Extended Reconstruction Sea Surface Temperature data set, version 5, NOAA
GIS: geographic information system
GLIMS: Global Land Ice Measurements from Space, National Snow and Ice Data Center, USA
Landsat 1/2/4-MSS: Landsat 1–4 multispectral scanner
NOAA: National Oceanic and Atmospheric Administration, USA
NZA: Novaya Zemlya Archipelago
SST: sea-surface temperature
WGS: World Geodetic System

To access the supplementary material, please visit the article landing page

Introduction

Retreating glaciers are an important indicator of global warming and a significant contributor to sea-level rise. Glacier-change chronologies show an increasing trend in mass loss over the last two decades throughout the world (Fox-Kemper et al. 2021). Glaciers in the Russian High Arctic represent about 10% of the world's glacier ice mass, excluding the Antarctic and Greenland ice sheets (Vaughan et al. 2013). Some global models project sea-level rise contributions from Russian High-Arctic glaciers ranging from 5 to 20 mm in sea-level equivalent by 2100, similar to projected sea-level equivalent contributions from glaciers in the region defined in the Randolph Glacier Inventory as Arctic Canada South (mainly Baffin Island) and Svalbard and glaciers along the periphery of Antarctica and Greenland (Radić et al. 2014; Marzeion et al. 2020; Rounce et al. 2023). The Arctic is a critical bellwether for climate change study as Arctic amplification results in air temperature increases at double the global average rate (Screen & Simmonds 2010; IPCC 2018). With a projected temperature increase of 1.5°C by 2052 (2018 baseline) in the Arctic, indigenous peoples and coastal communities along with tundra habitat and wildlife will be at a disproportionately higher risk of adverse effects (Tape et al. 2016; IPCC 2018; Berner et al. 2020).

Among the glaciated areas of the Russian High Arctic, the NZA experienced about 80% (–7.1 ± 1.2 Gt a^{-1}) of total glacier mass loss from 2003 to 2009 (Moholdt et al. 2012; Sommer et al. 2020). The NZA is the largest and southernmost glaciated area in the Russian High Arctic (GLIMS & NSIDC 2005). The northern island (Severny Island) is separated from the southern island (Yuzhny Island) by the Matochkin Strait, which connects the Kara Sea to the east and the Barents Sea to the west (Fig. 1).

Citation: *Polar Research* 2025, *44*, 10778, http://dx.doi.org/10.33265/polar.v44.10778

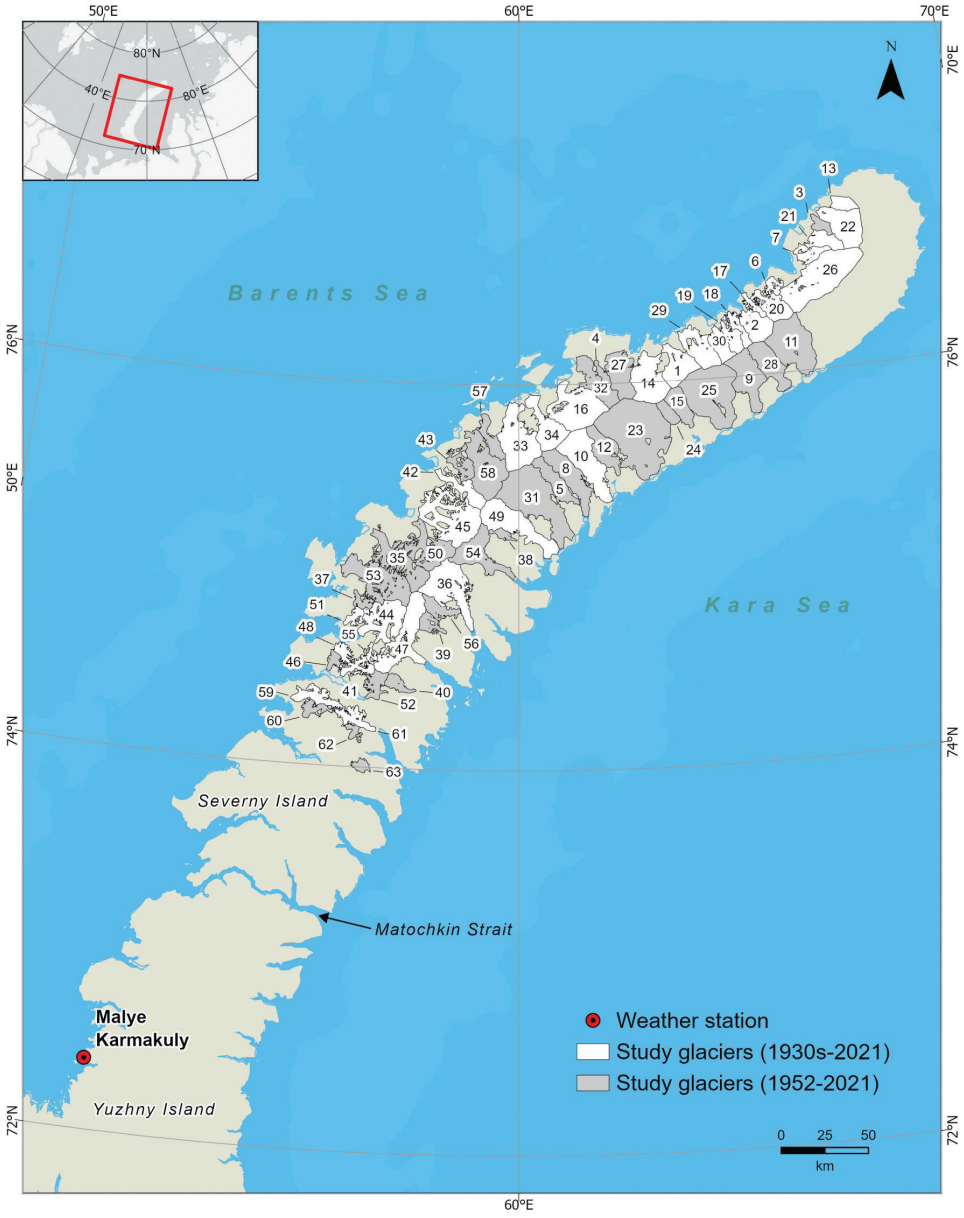

Fig. 1 The location of the 63 study glaciers and the Malye Karmakuly weather station in Novaya Zemlya. The subset of 31 glaciers with length change records extending back to the 1930s are shown in white.

The mountain range along the spine of the NZA has a maximum altitude of 1600 m on Severny Island, where an ice cap comprises over 90% of the total glaciated area in the NZA. Outlet glaciers extend from the ice sheet toward the Barents and Kara seas as land-, lake- and marine-terminating glaciers. The glaciers on the narrow Severny Island are all close to either the Kara Sea or the Barents Sea, exposing the glaciers to warmer coastal temperatures and ocean currents in the Arctic summer months. The region is dominated by larger glaciers, including 49 glaciers larger than 100 km^2, covering 84% of the total glacier area (22 379 km^2), according to a new glacier inventory by Rastner et al. (2017).

The North Atlantic-derived waters of the Barents Sea influence the climate in the NZA, and the mountains provide an orographic barrier for eastward moving North Atlantic systems. Peak precipitation rates occur in August and the lowest rates occur in April, with the highest winter accumulations occurring from October to January. Average monthly temperatures (1992–2021) recorded at the Malye Karmakuly weather station (Fig. 1) peak in July (7.7°C) and are above freezing in June (3.1°C), August (7.0°C) and

Citation: *Polar Research* 2025, *44*, 10778, http://dx.doi.org/10.33265/polar.v44.10778

September (4.3°C). Annual average temperatures decrease from about –5°C in the south-west to about –10°C in the north-east (Zeeberg & Forman 2001).

The history of glacier change in the NZA prior to the 21st century is not well-understood compared to other regions in the world (Sharov 2005; Moholdt et al. 2012; Rastner et al. 2017). After the Second World War, the Soviet Union designated the NZA as a test range for nuclear weapons, essentially closing the remote region to field research until the last bomb test was performed in 1990 (Zeeberg 2001). Most glacier change studies in the NZA have involved either small glacier sample sizes (e.g., Zeeberg & Forman 2001) or temporal extents of less than 20 years (e.g., Moholdt et al. 2012; Gardner et al. 2013; Sun et al. 2017; Ciracì et al. 2018; Tepes et al. 2021). Some studies show that ice dynamics and calving flux play an important role in the NZA as marine-terminating glaciers are retreating and thinning faster than land-terminating glaciers (Carr et al. 2014; Melkonian et al. 2016; Ciracì et al. 2018; Kochtitzky et al. 2022; Carr et al. 2023). Others conclude that glaciers on the Barents Sea coast have higher thinning and retreat rates compared to those along the Kara Sea coast (Sharov 2005; Moholdt et al. 2012; Carr et al. 2014; Melkonian et al. 2016). To better understand the complex relationships between climate, ocean forcing and glacier change, and given the importance of this region in terms of its future contribution to sea-level rise, it is necessary to study the history of glacier change in the NZA over longer timeframes and with greater temporal resolution.

In this article, we present the longest decadal chronology of glacier change in the NZA to date, and compare glacier change trends based on terminus type (land-, lake- or marine-terminating) and whether they terminate near the Barents Sea or the Kara Sea. The glacier chronology includes a 90-year record (ca, 1931–2021) of frontal length change and a 70-year record (1952–2021) of glacier area change for the 63 largest outlet glaciers, representing 86% of the NZA's total ice mass. We compared glacier changes to previous observations and changes in climate and SST to gain insight on potential forcings on glacier variation in the NZA.

Data and methods

The decadal glacier chronology is based on interpretations of survey records (1930s), digitized historical topographic maps (1952) and satellite imagery from the 1960s to 2021. We manually digitized the complete glacier outlines of the 63 largest outlet glaciers using maps and satellite images representing the years 1952, 1961, 1973, 1980, 1991, 2001, 2011 and 2021. Soviet expedition surveys (Chizov et al. 1968) provided glacier front position change measurements, extending the chronology back to the early 1930s for a subset of the study glaciers (Fig. 1). Supplementary Fig. S1 shows an excerpt of the glacier position change summary table from Chizov et al. (1968). The chronology of glacier outlines provided the data necessary to measure frontal length changes and changes in total glacier area and lower glacier area (including the glacier terminus and lower lateral margins). The general characteristics of each glacier are provided in Table 1.

Data acquisition and processing

Digitally scanned Soviet military topographic maps provided the spatial data needed to extend the glacier length chronology to 1952. The 16 topographic maps used in this study were obtained from an online database of historical Soviet era maps (https://maps.vlasenko.net/). The list of topographic maps is included in Supplementary Table S1. The maps were produced at the 1:200 000 scale from aerial photographs acquired in 1952 and updated in 1971, with the 1952 glacier positions retained (Zeeberg 2001). We georeferenced the maps using polynomial transformations and ground control points derived from orthorectified satellite images and projected the maps into the North Pole Lambert Azimuthal Equal Area coordinate system with WGS 1984 datum. Glacier front change measurements summarized by Chizov et al. (1968), based on Soviet topographic maps and field surveys, extended our frontal length change chronology back to the early 1930s for a subset of 31 study glaciers.

We acquired georeferenced and orthorectified satellite images from the US Geological Survey Earth Explorer website (https://earthexplorer.usgs.gov/), including images captured from Landsat 1/2/4-MSS (1973; 1980–1983), the Landsat 5 thematic mapper sensor (1991) and the Landsat 7 Enhanced Thematic Mapper Plus sensor (2001; 2010–2011). Sentinel-2 satellite images were obtained from the Copernicus Open Access Hub (https://scihub.copernicus.eu/dhus/#/home) to digitize glacier outlines for the year 2021. The list of the 70 satellite images obtained for this study is included in Supplementary Table S1. We used false colour composites of bands during the manual glacier outline digitizing process to provide contrast between ice, rock and water. To digitize glacier outlines representing the early 1960s, 18 declassified Corona spy satellite images from missions KH-2 (1961) and KH-4 (1962) were obtained from the US Geological Survey Earth Explorer website. The Corona images were orthorectified using the high-resolution ArcticDEM surface model (Porter et al. 2018), georeferenced using ground control points derived from orthorectified satellite images, and

Table 1 General characteristics of the study glaciers.

Map ID	GLIMS ID	Name	Terminus type	Latitude (centroid) (°)	Longitude (centroid) (°)	Mean altitude (m a.s.l.)	Area (km^2)	Avg slope (%)	Aspect (°)
1	G063362E76059N	Chasva	Marine	76.07	63.37	762	308	1.3	238
2	G065077E76240N	Brounova	Marine	76.25	65.10	585	253	5.8	219
3	G066649E76746N		Lake	76.74	66.73	363	77	5.1	257
4	G061696E76079N		Land	76.05	61.78	538	61	4.1	252
5	G060625E75546N		Land	75.50	60.73	659	241	3.1	115
6	G065659E76423N	Karbasnikova	Land	76.45	65.55	407	72	12.8	227
7	G066577E76580N	Pavlova	Marine	76.60	66.41	405	130	8.3	204
8	G061098E75482N		Land	75.52	61.04	615	385	2.8	113
9	G064799E76021N		Marine	75.99	64.82	548	432	2.8	103
10	G061273E75654N	Kropotkina	Marine	75.60	61.38	624	562	3.0	110
11	G065535E76176N		Marine	76.14	65.84	496	620	2.9	100
12	G061637E75691N		Land	75.66	61.76	587	274	4.3	106
13	G067122E76843N	Petersieva	Lake	76.83	67.28	607	101	1.9	240
14	G062464E75974N	Shokal'skogo	Marine	76.01	62.74	714	452	2.5	231
15	G063303E75842N		Land	75.87	63.37	587	203	2.9	93
16	G061252E75863N	Chernysheva	Marine	75.88	61.21	628	576	4.7	230
17	G065159E76339N	Anuchipa	Marine	76.36	65.07	491	64	12.0	237
18	G064547E76265N	Voikova	Marine	76.25	64.73	603	106	6.0	241
19	G064411E76256N	Maka	Marine	76.20	64.57	656	134	5.3	220
20	G065569E76336N	Vize	Marine	76.35	65.51	540	229	8.0	231
21	G066879E76643N	Vera	Marine	76.65	66.77	524	160	7.2	233
22	G067156E76738N	Boongeh	Marine	76.72	67.24	721	395	1.6	237
23	G062382E75725N		Marine	75.73	62.45	581	1,249	2.8	109
24	G063105E75839N		Land	75.83	63.11	623	99	3.0	78
25	G063849E75923N		Marine	75.92	64.04	581	838	2.6	112
26	G066985E76524N	Inostrantseva	Marine	76.47	66.59	529	826	5.6	193
27	G062285E76039N		Land	76.05	62.15	753	338	2.3	251
28	G065516E75995N		Marine	76.05	65.31	502	323	3.0	101
29	G064054E76109N	R'ikacheva	Marine	76.16	63.85	816	310	1.1	230
30	G064423E76139N	Vyolkena	Marine	76.17	64.31	726	163	3.4	229
31	G059699E75391N		Marine	75.40	60.33	908	900	1.3	111
32	G061854E75934N		Marine	76.01	61.63	849	297	1.6	236
33	G060115E75811N	Krainii	Marine	75.71	59.98	486	584	4.9	230
34	G060381E75794N	Taisia	Marine	75.78	60.58	643	332	3.7	240
35	G057304E75140N		Marine	75.08	57.64	576	414	7.1	203
36	G058678E75023N	Oga	Land	74.94	58.64	721	565	2.6	112
37	G056831E74854N		Lake	74.86	56.96	507	71	9.4	227
38	G059590E75223N		Land	75.23	59.68	869	54	1.3	86
39	G058182E74768N	Slim	Land	74.76	58.28	580	104	4.8	108
40	G057645E74442N	Ladigina	Land	74.44	57.69	541	95	5.3	115
41	G056734E74500N	Northern	Lake	74.52	56.93	546	131	13.4	181
42	G059176E75430N	Vilkitskovo	Marine	75.46	58.86	603	227	7.8	212
43	G058625E75597N		Marine	75.59	58.84	414	157	10.6	196
44	G057682E74831N	Pakrya	Land	74.77	57.39	423	414	7.5	153
45	G058922E75263N	Nordelshelda	Marine	75.31	58.65	571	670	7.0	199
46	G056467E74556N		Lake	74.54	56.47	416	60	8.4	148
47	G057408E74539N	Hammer & Sickle	Marine	74.69	57.80	736	527	1.8	129
48	G056632E74594N	Bulya	Land	74.59	56.64	483	76	9.1	246
49	G059995E75258N	Vilki (Nansena)	Marine	75.28	59.92	910	548	1.5	106
50	G057928E75129N		Lake	75.15	58.21	623	379	7.6	199
51	G056819E74779N	Wide	Land	74.78	56.82	435	73	10.4	176
52	G057314E74437N		Lake	74.43	57.29	553	143	7.7	130

(Continued)

Citation: *Polar Research* 2025, *44*, 10778, http://dx.doi.org/10.33265/polar.v44.10778

Table 1 (continued) General characteristics of the study glaciers.

Map ID	GLIMS ID	Name	Terminus type	Latitude (centroid) (°)	Longitude (centroid) (°)	Mean altitude (m a.s.l.)	Area (km²)	Avg slope (%)	Aspect (°)
53	G057661E74953N		Marine	74.97	57.26	476	569	7.0	208
54	G059092E75148N		Marine	75.12	59.21	769	391	2.3	129
55	G057173E74587N	Unior	Land	74.59	57.17	835	48	39.9	218
56	G058556E74798N		Land	74.84	58.44	655	144	3.6	105
57	G059401E75657N		Lake	75.72	59.42	509	158	4.5	230
58	G059108E75722N		Marine	75.57	59.32	682	549	4.1	214
59	G056555E74333N	Loud	Lake	74.35	56.17	451	185	7.0	191
60	G056096E74285N		Land	74.29	56.15	413	94	7.1	176
61	G056927E74274N	Vitte	Marine	74.25	56.92	502	153	7.4	128
62	G056933E74173N	Reingardta	Land	74.18	56.92	367	49	8.6	160
63	G057161E74006N		Land	74.01	57.09	561	57	8.0	152

projected into the North Pole Lambert Azimuthal Equal Area coordinate system with World Geodetic System 1984 datum. To improve the accuracy of glacier outlines, we obtained satellite images acquired late in the ablation season, between July and late September, when the seasonal snow cover was less likely to obscure glacier margins. Because of the limited availability of usable images in the early 1960s and 1970s, some images acquired before and after the ablation season were used to complete the glacier chronologies. The resolution of the satellite images ranged from 2 to 60 m and provided the spatial data for the decadal measurement of glacier outlines spanning 1961–2021.

We acquired climate data for the coastal Malye Karmakuly weather station (72.37°N, 52.73°E, 16 m a.s.l.; Fig. 1) from the NOAA Climate Data Online service and air temperature anomaly data from NOAA's Merged Land Ocean Global Surface Temperature Analysis data set (NOAAGlobalTemp; Zhang et al. 2019). NOAA's ERSSTv5 global monthly 2° ×2° grid SST data set was used to construct SST time series (See our supplementary climate time series methodology for ERSSTv5 grid locations). Reanalysis of the ERSSTv5 data set involved combining ship-based and buoy-based observations to reconstruct historical sea-surface temperatures (Huang et al. 2017).

Measurement of glacier changes

Digitized NZA glacier outlines developed by Rastner et al. (2017) were obtained from the GLIMS database (Raup et al. 2007) and provided the initial glacier boundaries. For each glacier chronology period, we manually digitized and adjusted complete glacier boundaries and margins based on the interpretation of topographic maps and satellite images representative of each period (see Fig. 2 for examples of digitized terminal positions). Source image metadata for each glacier outline include image platform, identification, spatial resolution and collection date. General physical characteristics, including glacier name (if available), GLIMS ID, centroid coordinates, glacier terminus type (lake, land or marine) and altitude (mean, minimum and maximum) are also included in the metadata. The digitized NZA glacier outlines are available from the GLIMS database (www.glims.org).

We measured changes in length, total area and lower glacier area between each chronology period for all 63 study glaciers using GIS geoprocessing tools. The outline method (Black & Kurtz 2022) was used to measure change in lower glacier area or the ice area including the glacier terminus and lower lateral margins (see Supplementary Fig. S2a). The outline method measures the area down-glacier from an arbitrary reference line intersecting the glacier above the lateral and frontal margins of the terminus. Measuring both total area and lower glacier area provided the data needed to assess the contribution of area losses at the lower glacier margins to the overall glacier area loss. Glacier centre lines were calculated from the highest point of the glacier to the terminus using a semi-automatic, GIS-based algorithm (Le Bris & Paul 2013) and high-resolution ArcticDEM elevation data. Changes in glacier length across chronology periods were calculated as the distance between each glacier terminus measured along the centre line, and relative changes calculated as the percentage of change relative to glacier lengths in 1952. Glacier area and length change rates for each period were calculated for all glaciers and by glacier terminus type.

Accuracy assessment

Several factors contribute to uncertainty when using satellite imagery in glacier studies, including image quality, resolution, georeferencing issues and analyst editing errors and skill in distinguishing glacier features (Racoviteanu et al. 2009; Paul et al. 2013; Paul & Mölg 2014; Pfeffer et al.

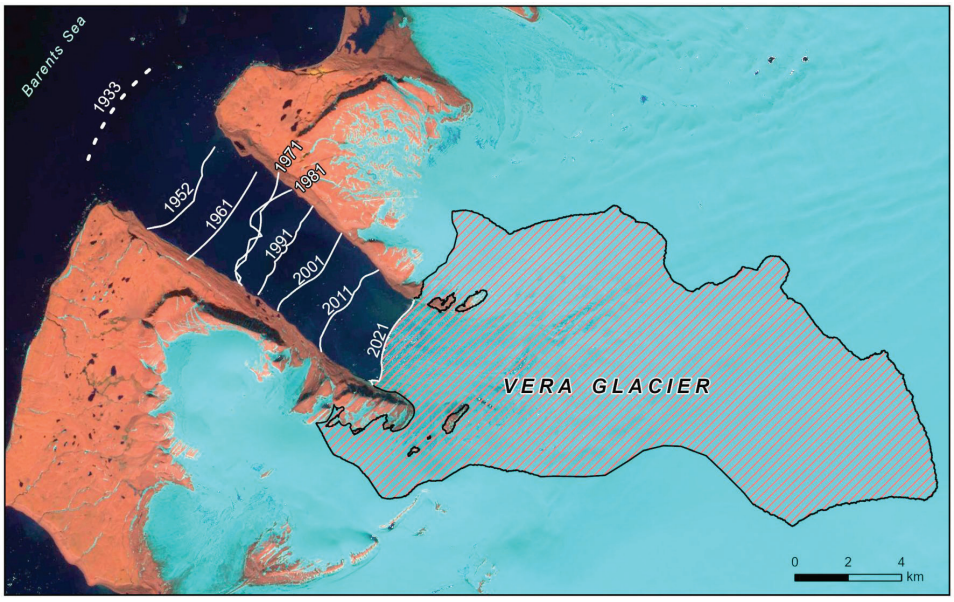

Fig. 2 Sentinel-2 image from 2021 with digitized terminal positions for Vera Glacier. The dashed white line indicates the 1933 terminus position from Chizov et al. (1968).

2014; Rastner et al. 2017). The following steps were taken to minimize errors: (1) selected satellite images without significant cloud cover or shadows along glacier margins; (2) acquired late summer (July-September) images to minimize seasonal snow; (3) obtained georeferenced and orthorectified satellite images and (4) checked for geolocation errors. Orthorectified images from Landsat 1/2/4-MSS were georeferenced against Sentinel-2 images from 2021 to assess the quality of the older images. The resulting root mean square error for the older Landsat images used in the study ranged between 30 and 61 m. Debris cover, a common challenge in glacier studies, was not a significant issue among the 63 study glaciers.

Glacier outlines and terminus positions were assumed to be accurate to ± 1 image pixel for Corona, Landsat and Sentinel-2 images. Zeeberg (2001) estimated a horizontal accuracy of 100–200 m for the Soviet military topographic maps on the basis of position location comparisons with Corona satellite images from 1964 and synthetic aperture radar images from 1993. We further assessed the accuracy and precision of digitized glacier outlines following methods recommended by Paul et al. (2017), including multiple digitizing and literature values. The multiple digitizing method tests the precision (uncertainty) associated with the analyst's manual digitization skills. The method involved the selection of six study glaciers and three rounds of manual glacier outline digitizing and area calculation, conducted on separate days, for each glacier. The precision for the calculated area of all six glaciers ranged from 0.3 to 6.1%, with an average of 3.0% of area measured. By comparison, literature values for digitizing glacier outline accuracy range from about 2 to 5% of the area measured (Paul et al. 2013; Bajracharya et al. 2014; Fischer et al. 2014; Paul & Mölg 2014; Pfeffer et al. 2014).

Climate and SST analysis

We developed precipitation and air temperature time series for the Malye Karmakuly weather station and constructed regional air temperature anomaly time series using the NOAAGlobalTemp reanalysis data set (hereafter referred to as the reanalysis data set). These data were then used to visually assess the relationships with glacier changes over time. Summer SST time series were constructed from the ERSSTv5 data set for open water grids along the Barents Sea and Kara Sea coasts to evaluate potential relationships between rising summer sea temperatures and the accelerated retreat of marine-terminating glaciers. Time series were developed for the months of June, July and August, and grouped into June–August and October–April averaging periods to represent the summer (ablation) and winter (accumulation) seasons in the Russian High Arctic. We applied distribution sampling and homogeneity testing, following Wijngaard et al. (2003), to assess the suitability of climate data sets for time series trend analysis, and used the Mann–Kendall trend test (Mann 1945; Kendall 1955) at a 5% significance level to detect trends (See our supplementary details regarding our time series

Citation: *Polar Research* 2025, *44*, 10778, http://dx.doi.org/10.33265/polar.v44.10778

methodology and techniques used to fill gaps in climate records).

Results

Length changes

The average frontal retreat rate for all 63 study glaciers increased each decade since the early 1970s, reaching a peak retreat rate of 65 m a^{-1} between 2011 and 2021 (Table 2). The lowest rate of frontal length retreat (9 m a^{-1}) occurred during the 1961–1973 period, when 62% of all study glaciers retreated. The lowest percentage of glaciers in retreat across all terminus types occurred during the period 1973–1980, with only 56% of all study glaciers retreating. Several glaciers displayed surge-type glacier characteristics, including rapid advance of several 100 m within a decade. Between 1961 and 1973, Maka Glacier, Inostrantsev Glacier and an unnamed glacier (Map ID 53) advanced over 1 km and Loud Glacier advanced 629 m (length change rates for individual glaciers are provided in Supplementary Table S2). Boongeh Glacier advanced 2.7 km and Hammer & Sickle Glacier advanced 626 m from 1981 to 1991. Chaeva Glacier advanced 655 m from 1973 to 1981. The percentage of study glaciers in retreat increased to 87–90% during the periods between 1991 and 2021. The fastest frontal retreat rates exceeded 250 ma^{-1} at the northern glaciers of Brounova and Inostrantsev between 1931 and 1952, and Maka and Boongeh glaciers from 1952 to 1961. Two unnamed and adjacent glaciers in the central portion of the study area exceeded the frontal retreat rate of 250 m a^{-1} during the 2001–2011 period (Map ID 43), and 2011–2021 period (Map ID 58).

Retreat rates varied significantly for different glacier terminus types. Land-terminating glaciers retreated at the slowest rate of the three types and peaked during the 2001–2011 period, with the mean rate of 18 m a^{-1} (14 m a^{-1} during 2011–2021; Fig. 3a). Lake-terminating glaciers reached peak frontal retreat rates (58 m a^{-1}) during the period 2011–2021 (Fig. 3b). Marine-terminating glaciers retreated at increasing rates since the 1970s, with a peak rate of 96 m a^{-1} for the period 2011–2021 (Fig. 3c). For the period 2011–2021, glaciers terminating in the Barents Sea retreated at more than double the rate of those terminating in the Kara Sea (Fig. 3d–e). We observed the accelerated retreat rate of Barents Sea-terminating glaciers along the entire Barents coast (Fig. 4). Bulya Glacier, originally terminating in the Barents Sea, transitioned to land-terminating by the early 1980s and experienced declining retreat rates from its pre-transition peak of 122 m a^{-1} (1952–1961) to 5 m a^{-1} from 2011 to 2021 (Supplementary Fig. S2b).

Table 2 Frontal length change and percent of glaciers in retreat across periods since 1952.

Glacier type	*N*	Metric	Period						
			1952–1961	1961–1973	1973–1980	1980–1991	1991–2001	2001–2011	2011–2021	1952–2021
All glaciers	63	Mean frontal length change (m a^{-1})	–51	–9	–10	–19	–33	–52	–65	–34
		Glaciers in retreat (%)	78	62	56	81	90	87	87	
Land-terminating	20	Mean frontal length change (m a^{-1})	–16	2	10	–13	–11	–18	–14	–9
		Glaciers in retreat (%)	55	40	35	70	80	70	75	
Lake-terminating	9	Mean frontal length change (m a^{-1})	–32	–7	–29	–23	–52	–43	–58	–35
		Glaciers in retreat (%)	89	67	78	100	89	89	89	
All marine-terminating	34	Mean frontal length change (m a^{-1})	–76	–17	–16	–21	–40	–75	–96	–49
		Glaciers in retreat (%)	88	74	62	82	97	97	94	

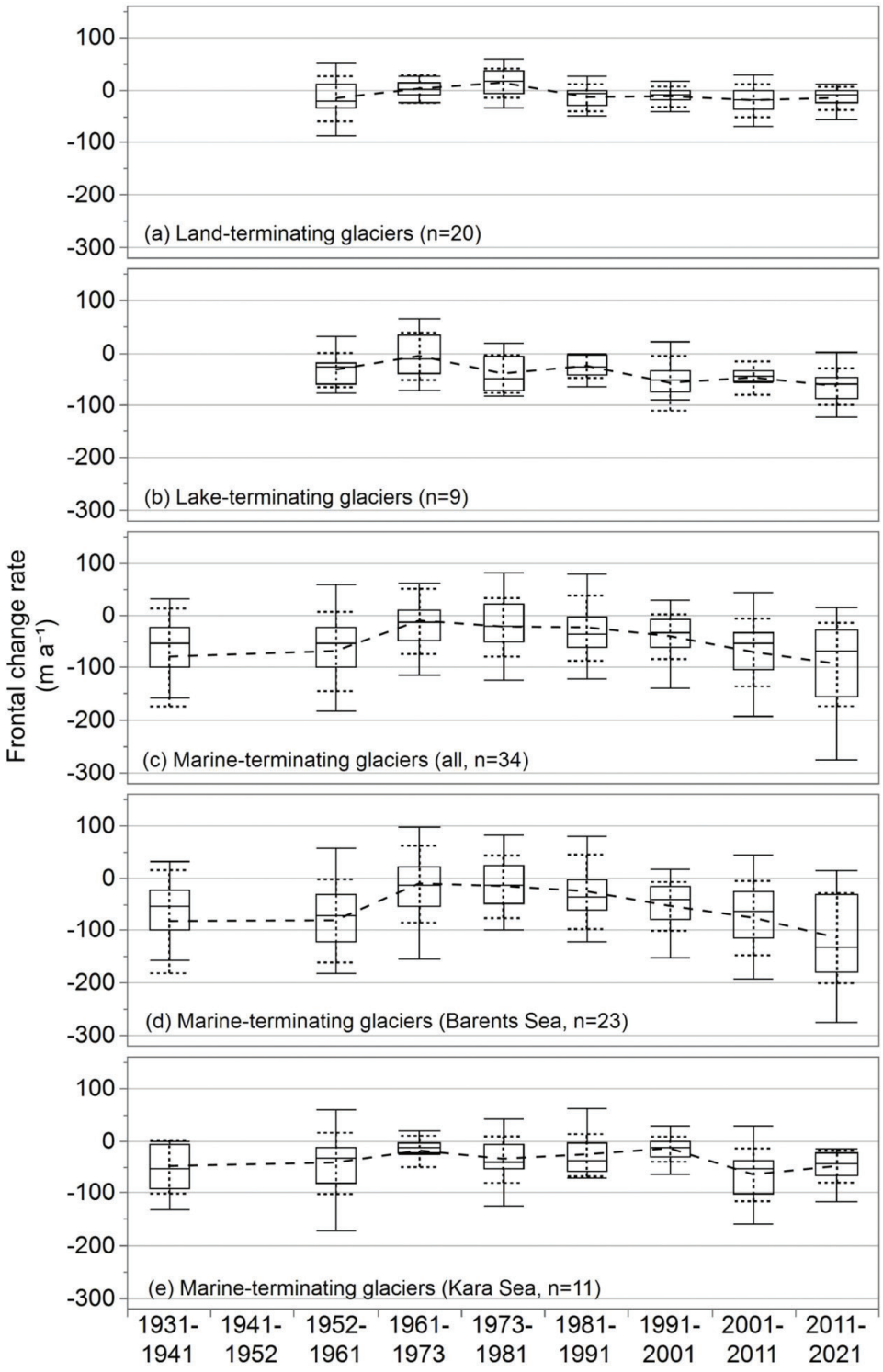

Fig. 3 Box plots of frontal change rates by glacier type. Horizontal lines indicate the median, dashed lines cross the means and the top and bottom edges of boxes represent the 25th and 75th percentiles. Whiskers span the range of data points, excluding outliers. Dotted error bars were constructed using one standard deviation from the mean.

Citation: *Polar Research* 2025, *44*, 10778, http://dx.doi.org/10.33265/polar.v44.10778

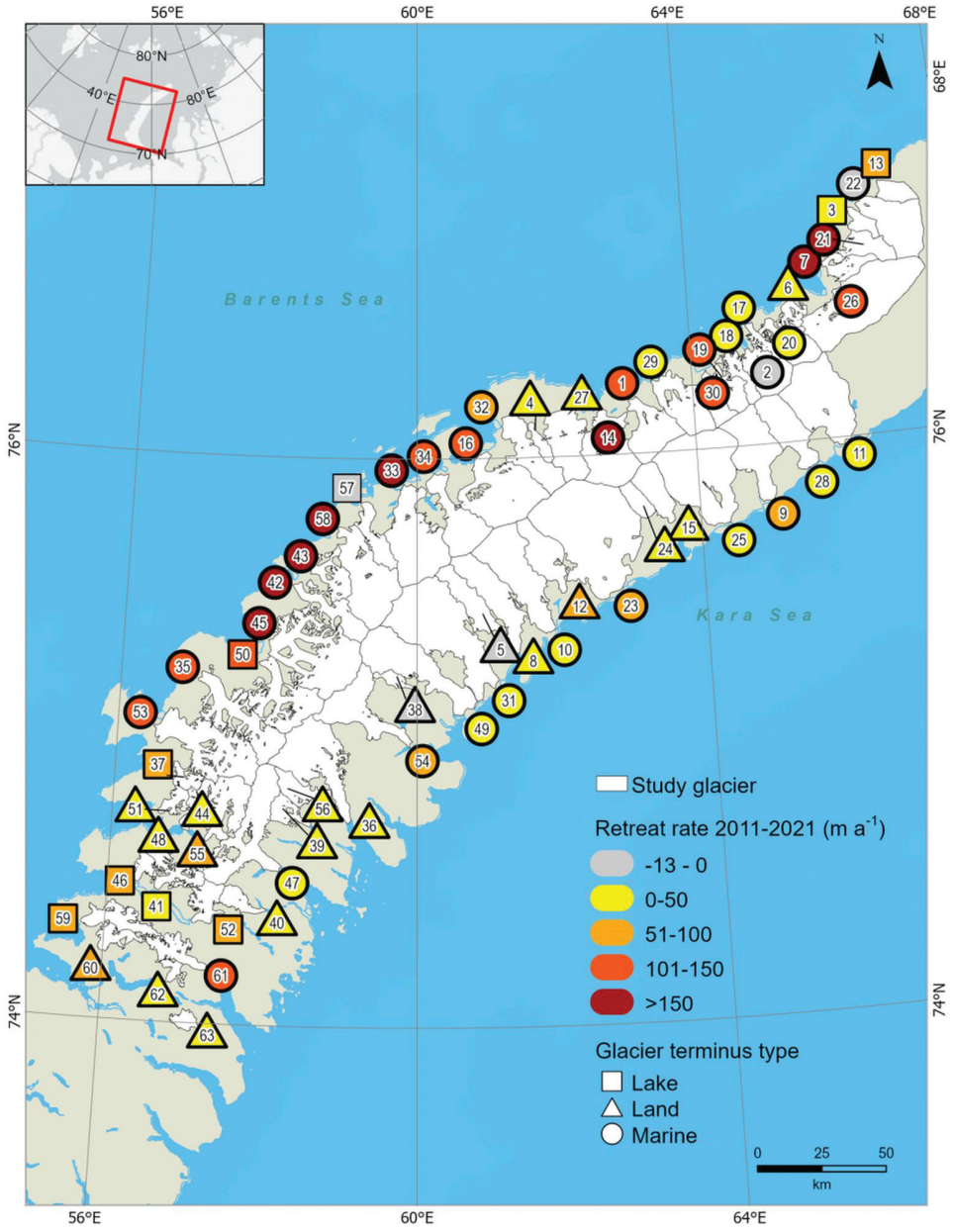

Fig. 4 Frontal change rates from 2011 to 2021 by glacier terminus type. Glacier map identification numbers (see Table 1) are included within the glacier type symbols.

After a period of rapid retreat across all glacier terminus types from 1952 to 1961, frontal retreat slowed among marine- and lake-terminating glaciers during the period 1961–1973, and land-terminating glaciers advanced slightly, on average, from 1961 to 1980. In terms of relative frontal length change since 1952, study glaciers lost an average of 2.6 km (8.2%) of total length from 1952 to 2021 (Fig. 5a, c). Lake-terminating glaciers retreated an average of 2.7 km (11.2%), and land-terminating glaciers lost only 0.7 km (3.7%) of total length since 1952. Glaciers terminating in the Barents Sea experienced the greatest length losses, retreating an average of 4.2 km (11.6%) since 1952.

Additional glacier terminus measurements obtained from Soviet expedition surveys extended the length change chronology of 31 glaciers back to 1931–35. The observations from this subset of glaciers indicate a period a rapid frontal retreat (75 m a^{-1}) for all marine-terminating glaciers from 1931 to 1952, second

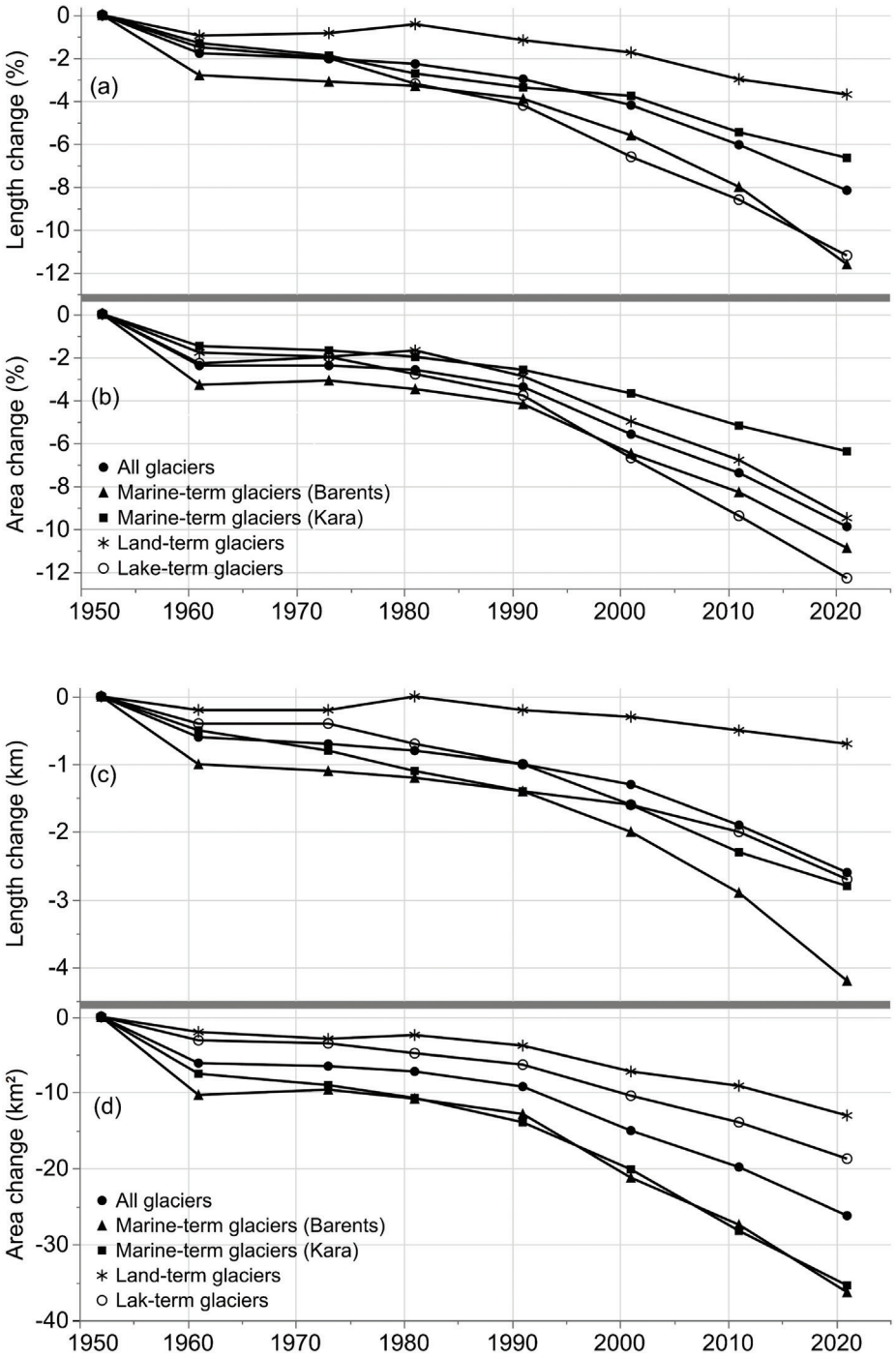

Fig. 5 Average cumulative percent (a) length change and (b) area change by glacier type, from the 1952 baseline length; average cumulative (c) length change and (d) area change by glacier type, from the 1952 baseline length.

Citation: *Polar Research* 2025, *44*, 10778, http://dx.doi.org/10.33265/polar.v44.10778

only to the period 2011–2021 in terms of highest rate of retreat (86 m a^{-1}; Fig. 3c; Supplementary Table S3). However, the calculated standard deviation for retreat rates suggests a higher degree of uncertainty for the 1931–1952 interval (Fig. 3c–e). For the period 1952–2021, the frontal length change and percentage of glaciers in retreat statistics for this subset reflect the general trends found among all study glaciers.

To better understand the potential drivers for frontal changes in the NZA, we calculated the Pearson's correlation coefficient between changes in climate variables and frontal changes from 1952 to 2021 (Supplementary Table S4). Results demonstrate the strongest negative correlations between change rates for Barents Sea-terminating glaciers and increased summer SSTs in both the Barents Sea (r = -0.57, p < 0.0001) and Kara Sea (r = -0.61, p < 0.0001). June SSTs in the Kara Sea show the strongest negative relationship, with frontal change in glaciers terminating in the Kara (r = -0.56, p < 0.0001) and Barents Seas (r = -0.66, p < 0.0001). Significant but moderate relationships were observed between frontal change in glaciers terminating in the Barents Sea and winter precipitation (r = 0.43, p = 0.000), summer temperature anomaly (r = -0.49, p < 0.0001) and June air temperature (r = -0.49, p < 0.0001). These results are consistent with the relationships observed between accelerating marine-terminating glacier retreat and significant increasing trends in summer air temperature and SSTs in recent decades (Fig. 6). Frontal changes in land-terminating glaciers correlate with June temperatures (r = -0.40, ρ = 0.001), June SSTs in the Kara Sea (r = -0.42, p = 0.000) and summer SSTs in the Kara Sea (r = -0.48, p < 0.0001).

Area changes

Over the period 1952–2021, study glaciers lost 1606 km^2 (10%) in total area, with the 34 marine-terminating glaciers accounting for 1221 km^2 (76%) of the total area loss (Table 3). Average total glacier area loss peaked during the period 2011–2021 for land- and lake-terminating glaciers. The largest total area loss for marine-terminating glaciers occurred during the period 1952–1961 (319 km^2), followed by a period of slow growth (2 km^2) between 1961 and 1973. Since the early 1970s, the total area of marine-terminating glaciers decreased across each decadal study period (Fig. 5b, d), with a peak decline of 283 km^2 from 2011 to 2021. Lower glacier area loss totalled 1026 km^2 or 64% of the total glacier area loss from 1952 to 2021. Marine-terminating glaciers accounted for 812 km^2 (79%) of the total lower glacier area loss, including 545 km^2 from Barents Sea-terminating glaciers and 267 km^2 from Kara Sea-terminating glaciers.

Discussion

The average rate of retreat for all 63 study glaciers in the NZA has increased over the last 50 years, peaking during the most recent study period from 2011 to 2021 (Table 2). The unprecedented rate of frontal retreat of all study glaciers from 2011 to 2021 is also reflected in the area change data with 406 km^2 of glacier area lost over the same period, representing 25% of the total glacier area loss since the early 1950s (Table 3). These findings are consistent with observations by Sommer et al. (2020) and Tepes et al. (2021), who noted accelerated glacier mass loss in the NZA since 2010.

The accelerating rate of marine-terminating glacier retreat in recent decades coincides with trends in climate and SSTs (Fig. 6a). We identified significant upward trends in summer surface air temperature at the Malye Karmakuly station, increasing by 0.2°C per decade from 1942 to 2021, and in air temperature anomaly (reanalysis data set), rising by 0.12°C per decade in the NZA from 1933 to 2021 (Fig. 6b–c). From 1991 to 2021, summer surface air temperature at the Malye Karmakuly station increased to 0.6°C per decade and air temperature anomaly (reanalysis data set), increased to 0.5°C per decade. Annual winter precipitation decreased 29% (11 mm per decade) from 1973 to 2021 (Fig. 6d). Average summer SSTs in the Barents and Kara seas increased 0.7°C per decade from 1990 to 2021 (Fig. 6e). Kara Sea SST data revealed June as an important month in terms of detecting the influence of warming on melting sea ice in the NZA. Consistently negative average June SSTs from 1930 to 1990 indicate sea-ice presence (Fig. 6f), with ERSSTv5 SST set to –1.8°C when grid sea-ice concentration exceeds 90% (Smith et al. 2008; Huang et al. 2017). This was followed by a notable increase in average June SSTs, rising by 1.4°C per decade from 1990 to 2021, signalling a significant shift to warmer, ice-free conditions. Overall, the trends in recently increasing air temperature and SST, and decreasing winter precipitation, suggest conditions appropriate for negative glacier mass balance and the observed accelerated retreat across the NZA.

Our analysis reveals a period of stability or slow retreat from the early 1960s into the early 1980s. This pattern is observed across all glacier types, with data from land-terminating glaciers even suggesting a period of advance, including increasing frontal length (Fig. 3a) and total glacier area (Table 3) from 1961 to 1981. We found no statistically significant trends in decreasing summer air temperatures or increasing winter precipitation at the Malye Karmakuly station from 1961 to 1981; however, years with cooler summer air temperatures and heavy winter precipitation were observed during this period (Fig. 6c–e). Zeeberg & Forman (2001) also reported a

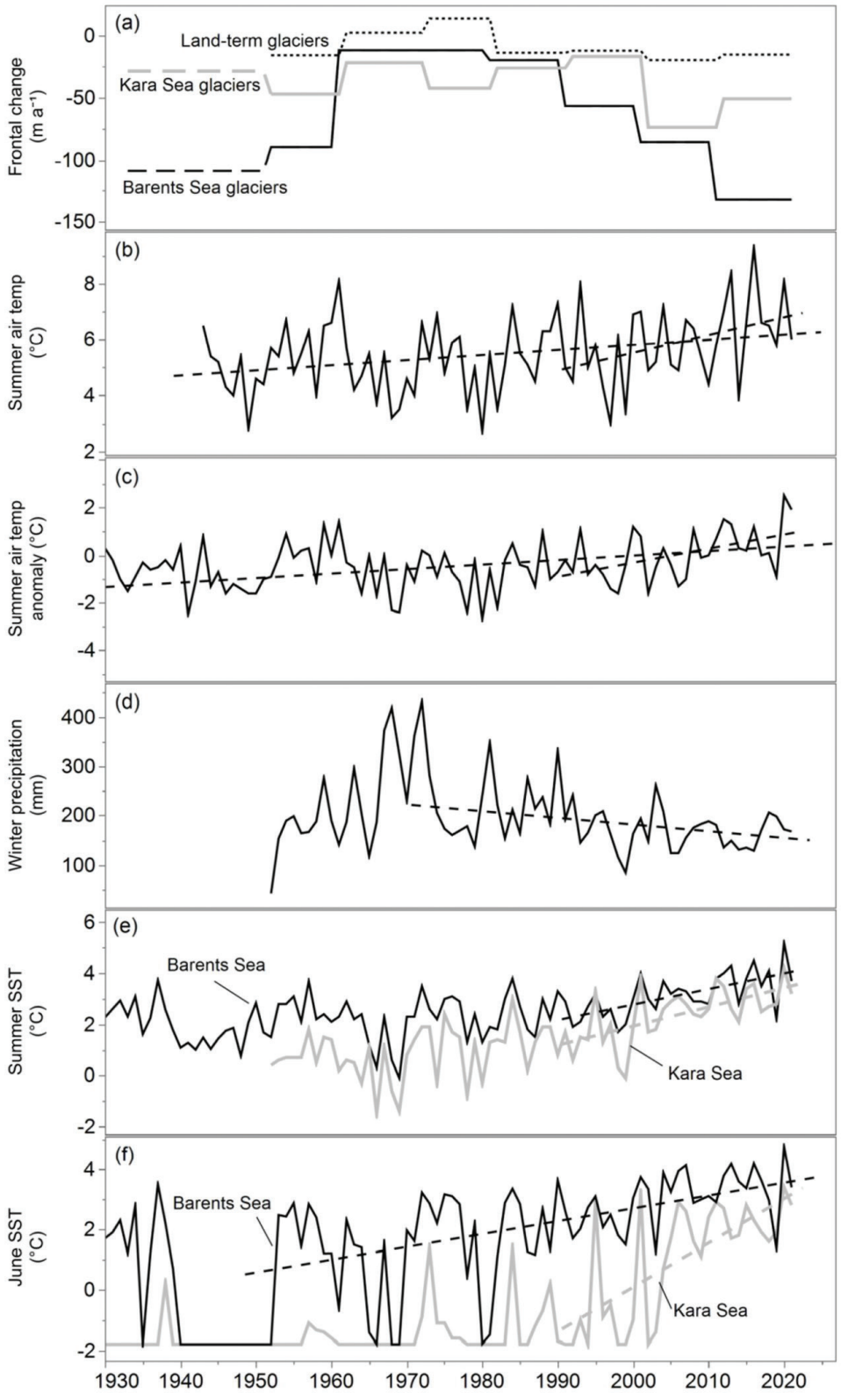

Fig. 6 Comparison between (a) glacier frontal change rates (dashed lines represent Soviet survey data); (b) summer air temperature (Malye Karmakuly weather station data); (c) summer air temperature anomaly (NOAA GlobalTemp data set); (d) winter precipitation (Malye Karmakuly weather station data); (e) summer SSTs (NOAA ERSSTv5 data set) and (f) June SSTs (NOAA ERSSTv5 data set). Dashed lines indicate statistically significant trends.

Citation: *Polar Research* 2025, *44*, 10778, http://dx.doi.org/10.33265/polar.v44.10778

Table 3 Total glacier area and lower area change across periods since 1952. Lower area change refers to the change in glacier area including only the glacier terminus and lower lateral margins (see Supplementary Fig. S2a).

Glacier type	*N*	Total area in 2021 (km²)	Metric (km²)	Period							
				1952–1961	1961–1973	1973–1980	1980–1991	1991–2001	2001–2011	2011–2021	1952–2021
All glaciers	63	19200	Total area change	–386	24	–46	–125	–365	–302	–406	–1606
			Total lower glacier area change	–243	–26	–51	–100	–143	–224	–239	–1026
			Total area change	–40	18	10	–29	–67	–38	–79	–225
Land-terminating	20	3446	Total lower glacier area change	–29	–2	8	–19	–18	–23	–24	–107
			Total area change	–28	4	–11	–13	–37	–31	–43	–160
Lake-terminating	9	1306	Total lower glacier area change	–12	–7	–12	–11	–20	–22	–23	–107
Marine-terminating	34	14448	Total area change	–319	2	–45	–83	–260	–233	–283	–1221
			Total lower glacier area change	–202	–17	–46	–70	–104	–179	–193	–812

period of glacier stability between 1964 and 1993 in the NZA, attributing positive glacier mass balance to the positive phase of the North Atlantic Oscillation index, increased SSTs in the Barents Sea and a rise in winter precipitation. Slow glacier retreat or stagnation between the 1960s and 1990s was also observed in other parts of the Arctic, including Greenland, Iceland and Svalbard (Howat & Eddy 2011; Błaszczyk et al. 2013; Belart et al. 2020). During this same period, seven glaciers displayed characteristics of surge-type glaciers. Three of these glaciers were categorized as either a confirmed surge-type glacier (Hammer & Sickle Glacier) or a glacier likely to have surged (Loud Glacier and unnamed glacier, Map ID 53) in a comprehensive study of surge-type glaciers in the NZA by Grant et al. (2009).

Since the 1980s, land-terminating glaciers retreated at a much slower rate compared to marine- and lake-terminating glaciers. However, the average rate of retreat of land-terminating glaciers from 2001 to 2021 (17.7 m a^{-1}) more than doubled the average rate of retreat across the last half of the 20th century (6.3 m a^{-1}). Larocca et al. (2023) documented similar results for land-terminating glaciers in Greenland, where the mean 21st century (ca. 2000–2021) frontal retreat rate of 14.8 m a^{-1} doubled the 20th century rate of 7.7 m a^{-1}. Compared to land-term inating glaciers, marine-terminating glaciers follow the same patterns of accelerated retreat after the early 1980s and peak retreat rates from 2011 to 2021. However, the retreat of marine-terminating glaciers increased at much higher rates, including six times the rate of retreat of land-terminating glaciers during the period 2011–2021 (Table 2). This suggests forces other than surface air temperature, including ocean forcing, are acting on marine-terminating glaciers in the NZA. This is further supported by the observed significant decline in retreat rate at Bulya Glacier after transitioning from marine-terminating to land-terminating in the early 1980s (Supplementary Fig. S2b). Carr et al. (2014) analysed the retreat rates of 38 glaciers in the NZA between 1992 and 2010 and reported similar findings, highlighting the fact that marine-terminating glaciers retreated at rates 10 times faster than land-terminating glaciers, partly due to changes in sea-ice concentration.

The warming waters of the Barents and Kara Seas enhance ablation at glacier margins through submarine melting and calving (Luckman et al. 2015; Tepes et al. 2021; Foss et al. 2024). June SST data represents early summer and shows a shift from recurring negative SSTs, indicating the presence of sea ice, to ice-free and warming conditions starting in the 1980s in the Barents Sea (Fig. 6f). This shift occurs much later in the Kara Sea (early 2000s). Glacier retreat rate data show a similar pattern as glaciers terminating in the Barents Sea

began retreating at an accelerated rate a decade earlier than glaciers terminating in the Kara Sea and at a much higher rate from 2011 to 2021 (Fig. 6a). Carr et al. (2014) and Tepes et al. (2021) observed a similar relationship between increasing SST, declining sea ice and accelerated glacier retreat in the NZA since the early 2000s. The highest average rates of retreat we observed were among glaciers terminating in the Barents Sea, consistent with previous findings that have suggested that the greatest glacier mass loss and highest retreat rates since the early 2000s occur on the Barents side of the NZA (Carr et al. 2014; Ciracì et al. 2018; Melkonian et al. 2016; Tepes et al. 2021). Since 1952, glaciers terminating in the Barents Sea experienced average length losses of 5.6% by 2001 and 11.6% by 2021, almost double the losses measured in Kara Sea-terminating glaciers. Sharov (2005) found similar results, observing a 6.6% loss in total length of nine marine-terminating glaciers on the NZA's Barents Sea coast from 1952 to 2001. Increased marine-terminating glacier retreat in recent decades is also observed elsewhere in the Arctic, including Greenland (Howat & Eddy 2011; King et al. 2020), Svalbard (Błaszczyk et al. 2013; Nuth et al. 2013) and the Canadian Arctic Archipelago (Noël et al. 2018).

The pattern of retreat for lake-terminating glaciers is similar to that of marine-terminating glaciers, with the lowest average retreat rates from 1961 to 1981, and the maximum average retreat rate (58 m a^{-1}) occurring from 2011 to 2021 (Table 2). Warming proglacial lakes accelerate frontal glacier retreat through mechanisms similar to ocean forcings, such as underwater melting and calving (Carrivick & Tweed 2013; Mallalieu et al. 2020; How et al. 2021).

The subset of 31 study glaciers included in Soviet field surveys have been retreating since the early 1930s, with a period of slow retreat between 1961 and 1980. From the early 1930s to 1952, 87% of the subset glaciers were in retreat at an average rate of 75 m a^{-1}, second only to the period 2011–2021, where 90% of the glaciers retreated with an average rate of 86 m a^{-1} (Fig. 6a; Supplementary Table S3). Of the 31 subset glaciers, 26 terminated in the Barents Sea (Fig. 1). Summer and June SST data for the Barents Sea suggest years with warmer temperatures from 1930 to 1940 (Fig. 6e-f). The lack of climate and SST data prior to 1930 makes it difficult to interpret trends and relationships with glacier change during the early part of the chronology. Greenland's glaciers displayed a similar pattern, with peak 20th century mass losses occurring in the first half of the century, coinciding with a period of warming, followed by accelerated mass loss from 2000 to 2022 (Kjeldsen et al. 2015; Larocca et al. 2023).

Conclusion

The complex interaction of climate and ocean forcings makes it difficult to explain the past variability and future response of any single glacier to continued Arctic warming. However, the high percentage of glaciers in retreat in the NZA since the early 1990s, combined with the total glacier area loss of 10% since the early 1950s, indicates a clear response to rising surface air and sea-surface temperatures. Accelerating glacier decline is evident, as the highest rates of glacier retreat and the greatest loss of glacier area among all glacier types occurred from 2011 to 2021, a period also experiencing peaks in summer surface air temperatures and summer and June SSTs, along with decreasing winter precipitation.

With the Russian High Arctic listed among the top regions in the world in terms of projected glacier volume loss in sea-level equivalent through 2100, we recommend continued monitoring of marine-terminating glaciers in the NZA. Marine-terminating glaciers, retreating since the early 1930s, account for the majority (76%) of the total glacier area loss in the NZA since 1952, and, as they continue to retreat, will eventually terminate on land. Further monitoring will help to calibrate and update glacier volume loss models by providing data on the behaviour of former marine-terminating glaciers, including whether some of them may readvance into the sea or continue to retreat at the slower rates observed among the land-terminating glaciers in this study.

Acknowledgements

The authors thank Anya Belan for her assistance with translating Russian text. The authors also sincerely appreciate the constructive comments from two anonymous reviewers.

Disclosure statement

The authors report no conflict of interest.

Funding

This research was supported by the Greater Milwaukee Foundation Mary Jo Read fellowship awarded to DRM.

References

Bajracharya S.R., Maharjan S.B. & Shrestha F. 2014. The status and decadal change of glaciers in Bhutan from the 1980s to 2010 based on satellite data. *Annals of Glaciology 55*, 159–166, doi: 10.3189/2014AoG66A125.

Belart J.M.C., Magnússon E., Berthier E., Gunnlaugsson Á.Þ., Pálsson F., Aðalgeirsdóttir G., Jóhannesson T., Thorsteinsson T. & Björnsson H. 2020. Mass balance of 14 Icelandic glaciers, 1945–2017: spatial variations and links with climate. *Frontiers in Earth Science 8*, article no. 163, doi: 10.3389/feart.2020.00163.

Berner L.T., Massey R., Jantz P., Forbes B.C., Macias-Fauria M., Myers-Smith I., Kumpula T., Gauthier G., Andreu-Hayles L., Gaglioti B.V., Burns P., Zetterberg P., D'Arrigo R. & Goetz S.J. 2020. Summer warming explains widespread but not uniform greening in the Arctic tundra biome. *Nature Communications 11*, article no. 4621, doi: 10.1038/s41467-020-18479-5.

Black T. & Kurtz D. 2022. Maritime glacier retreat and terminus area change in Kenai Fjords National Park, Alaska, between 1984 and 2021. *Journal of Glaciology 69*, 251–265, doi: 10.1017/jog.2022.55.

Błaszczyk M., Jania J.A. & Kolondra L. 2013. Fluctuations of tidewater glaciers in Hornsund Fjord (southern Svalbard) since the beginning of the 20th century. *Polish Polar Research 34*, 327–352, doi: 10.2478/popore-2013-0024.

Carr J.R., Stokes C. & Vieli A. 2014. Recent retreat of major outlet glaciers on Novaya Zemlya, Russian Arctic, influenced by fjord geometry and sea-ice conditions. *Journal of Glaciology 60*, 155–170, doi: 10.3189/2014JoG13J122.

Carr R., Murphy Z., Nienow P., Jakob L. & Gourmelen N. 2023. Rapid and synchronous response of outlet glaciers to ocean warming on the Barents Sea coast, Novaya Zemlya. *Journal of Glaciology*, e10, doi: 10.1017/jog.2023.104.

Carrivick J.L. & Tweed F.S. 2013. Proglacial lakes: character, behaviour and geological importance. *Quaternary Science Reviews 78*, 34–52, doi: 10.1016/j.quascirev.2013.07.028.

Chizov O., Koryakin V., Davidovich N., Kanevsky Z., Singer E., Bazheva V., Bazhev A. & Khmelevskoy I. 1968. Glaciation of the Novaya Zemlya. In: *Glaciology IX section of IGY Program 18.* P. 338. Moscow: Nauka. (In Russian, with English summary.)

Ciracì E., Velicogna I. & Sutterley T.C. 2018. Mass balance of Novaya Zemlya Archipelago, Russian High Arctic, using time-variable gravity from GRACE and altimetry data from ICESat and CryoSat-2. *Remote Sensing 10*, article no. 1817, doi: 10.3390/rs10111817.

Fischer M., Huss M., Barboux C. & Hoelzle M. 2014. The new Swiss glacier inventory SGI2010: relevance of using high-resolution source data in areas dominated by very small glaciers. *Arctic, Antarctic, and Alpine Research 46*, 933–945, doi: 10.1657/1938-4246-46.4.933.

Foss Ø., Maton J., Moholdt G., Schmidt L.S., Sutherland D.A., Fer I., Nilsen F., Kohler J. & Sundfjord A. 2024. Ocean warming drives immediate mass loss from calving glaciers in the High Arctic. *Nature Communications 15*, article no. 10460, doi: 10.1038/s41467-024-54825-7.

Fox-Kemper B., Hewitt H.T., Xiao C., Aðalgeirsdóttir G., Drijfhout S.S., Edwards T.L., Golledge N.R., Hemer M., Kopp R.E., Krinner G., Mix A., Notz D., Nowicki S., Nurhati I.S., Ruiz L., Sallée J.-B., Slangen A.B.A. & Yu Y. 2021. Ocean, cryosphere, and sea level change. In V. Masson-Delmotte et al. (eds.): *Climate change 2021: the physical science basis. Contribution of Working Group I to the sixth assessment report of the Intergovernmental Panel on Climate Change*. Pp. 1211–1362. Cambridge: Cambridge University Press.

Gardner A., Moholdt G., Cogley J., Wouters B., Arendt A., Wahr J., Berthier E., Hock R., Pfeffer W., Kaser G., Ligtenberg S., Bolch T., Sharp M., Hagen J., van den Broeke M. & Paul F. 2013. A reconciled estimate of glacier contributions to sea level rise: 2003 to 2009. *Science 340*, 852–857, doi: 10.1126/science.1234532.

GLIMS & NSIDC 2005. Global Land Ice Measurements from Space glacier database. Compiled and made available by the international GLIMS community and the National Snow and Ice Data Center, Boulder, CO. Accessed on the internet at https://www.glims.org/ on 1 April 2024

Grant K.L., Stokes C.R. & Evans I.S. 2009. Identification and characteristics of surge-type glaciers on Novaya Zemlya, Russian Arctic. *Journal of Glaciology 55*, 960–972, doi: 10.3189/002214309790794940.

How P., Messerli A., Mätzler E., Santoro M., Wiesmann A., Caduff R., Langley K., Bojesen M.H., Paul F., Kääb A. & Carrivick J.L. 2021. Greenland-wide inventory of ice marginal lakes using a multi-method approach. *Scientific Reports 11*, article no. 4481, doi: 10.1038/s41598-021-83509-1.

Howat I.M. & Eddy A. 2011. Multi-decadal retreat of Greenland's marine-terminating glaciers. *Journal of Glaciology 57*, 389–396, doi: 10.3189/002214311796905631.

Huang B., Thorne P.W., Banzon V.F., Boyer T., Chepurin G., Lawrimore J.H., Menne M.J., Smith T.M., Vose R.S. & Zhang H.-M. 2017. NOAA Extended Reconstructed Sea Surface Temperature (ERSST), version 5. Doi: 10.7289/V5T72FNM. Accessed on the internet at https://psl.noaa.gov/data/gridded/data.noaa.ersst.v5.html on 6 December 2023.

Intergovernmental Panel on Climate Change (IPCC) 2018. Summary for policymakers. In V. Masson-Delmotte et al. (eds.): *Global warming of 1.5°C. An IPCC Special Report on the impacts of global warming of 1.5°C above pre-industrial levels and related global greenhouse gas emission pathways, in the context of strengthening the global response to the threat of climate change, sustainable development, and efforts to eradicate poverty.* Pp. 3–24. Cambridge: Cambridge University Press.

Kendall M.G. 1955. *Rank correlation methods*. London: Griffin.

King M.D., Howat I.M., Candela S.G., Noh M.J., Jeong S., Noël B.P.Y., van den Broeke M.R., Wouters B. & Negrete A. 2020. Dynamic ice loss from the Greenland Ice Sheet driven by sustained glacier retreat. *Communications Earth & Environment 1*, article no. 1, doi: 10.1038/s43247-020-0001-2.

Kjeldsen K.K., Korsgaard N.J., Bjørk A.A., Khan S.A., Box J.E., Funder S., Larsen N.K., Bamber J.L., Colgan W., van den Broeke M., Siggaard-Andersen M.-L., Nuth C., Schomacker A., Andresen C.S., Willerslev E. & Kjær K.H. 2015. Spatial and temporal distribution of mass loss from the Greenland Ice Sheet since AD 1900. *Nature 528*, 396–400, doi: 10.1038/nature16183.

Kochtitzky W., Copland L., Van Wychen W., Hugonnet R., Hock R., Dowdeswell J.A., Benham T., Strozzi T., Glazovsky A., Lavrentiev I., Rounce D.R., Millan R., Cook A., Dalton A., Jiskoot H., Cooley J., Jania J. & Navarro F. 2022. The unquantified mass loss of Northern Hemisphere marine-terminating glaciers from 2000–2020.

Nature Communications 13, article no. 5835, doi: 10.1038/s41467-022-33231-x.

Larocca L.J., Twining–Ward M., Axford Y., Schweinsberg A.D., Larsen S.H., Westergaard–Nielsen A., Luetzenburg G., Briner J.P., Kjeldsen K.K. & Bjørk A.A. 2023. Greenland-wide accelerated retreat of peripheral glaciers in the twenty-first century. *Nature Climate Change 13*, 1324–1328, doi: 10.1038/s41558-023-01855-6.

Le Bris R. & Paul F. 2013. An automatic method to create flow lines for determination of glacier length: a pilot study with Alaskan glaciers. *Computers and Geosciences 52*, 234–245, doi: 10.1016/j.cageo.2012.10.014.

Luckman A., Benn D.I., Cottier F., Bevan S., Nilsen F. & Inall M. 2015. Calving rates at tidewater glaciers vary strongly with ocean temperature. *Nature Communications 6*, article no. 8566, doi: 10.1038/ncomms9566.

Mallalieu J., Carrivick J.L., Quincey D.J. & Smith M.W. 2020. Calving seasonality associated with melt-undercutting and lake ice cover. *Geophysical Research Letters 47*, e2019GL086561, doi: 10.1029/2019GL086561.

Mann H.B. 1945. Nonparametric tests against trend. *Econometrica 13*, 245–259, doi: 10.2307/1907187.

Marzeion B., Hock R., Anderson B., Bliss A., Champollion N., Fujita K., Huss M., Immerzeel W.W., Kraaijenbrink P., Malles J.-H., Maussion F., Radić V., Rounce D.R., Sakai A., Shannon S., van de Wal R. & Zekollari H. 2020. Partitioning the uncertainty of ensemble projections of global glacier mass change. *Earth's Future 8*, e2019EF001470, doi: 10.1029/2019EF001470.

Melkonian A.K., Willis M.J., Pritchard M.E. & Stewart A.J. 2016. Recent changes in glacier velocities and thinning at Novaya Zemlya. *Remote Sensing of Environment 174*, 244–257, doi: 10.1016/j.rse.2015.11.001.

Moholdt G., Wouters B. & Gardner A.S. 2012. Recent mass changes of glaciers in the Russian High Arctic. *Geophysical Research Letters 39*, L10502, doi: 10.1029/2012GL051466.

Noël B., van de Berg W.J., Lhermitte S., Wouters B., Schaffer N. & van den Broeke M.R. 2018. Six decades of glacial mass loss in the Canadian Arctic Archipelago. *Journal of Geophysical Research—Earth Surface 123*, 1430–1449, doi: 10.1029/2017JF004304.

Nuth C., Kohler J., König M., Von Deschwanden A., Hagen J.O., Kääb A., Moholdt G. & Pettersson R. 2013. Decadal changes from a multi-temporal glacier inventory of Svalbard. *Cryosphere 7*, 1603–1621, doi: 10.5194/tc-7-1603-2013.

Paul F., Bolch T., Briggs K., Kääb A., McMillan M., McNabb R., Nagler T., Nuth C., Rastner P., Strozzi T. & Wuite J. 2017. Error sources and guidelines for quality assessment of glacier area, elevation change, and velocity products derived from satellite data in the Glaciers_cci project. *Remote Sensing of Environment 203*, 256–275, doi: 10.1016/j.rse.2017.08.038.

Paul F. & Mölg N. 2014. Hasty retreat of glaciers in northern Patagonia from 1985 to 2011. *Journal of Glaciology 60*, 1033–1043, doi: 10.3189/2014JoG14J104.

Paul F., Winsvold S., Le Bris R., Scharrer K., Bolch T., Barrand N.E., Frey H., Rastner P., Steffen S., Raup B., Konovalov V., Nosenko G., Joshi S.P., Racoviteanu A., Nuth C., Pope A., Mölg N., Baumann S., Casey K. & Berthier E. 2013. On the accuracy of glacier outlines derived from remote-sensing data. *Annals of Glaciology 54*, 171–182, doi: 10.3189/2013aog63a296.

Pfeffer W.T., Arendt A.A., Bliss A., Bolch T., Cogley J.G., Gardner A.S., Hagen J.O., Hock R., Kaser G., Kienholz C., Miles E.S., Moholdt G., Mölg N., Paul F., Radić V., Rastner P., Raup B.H., Rich J., Sharp M.J., Andreassen L.M., Bajracharya S., Barrand N.E., Beedle M.J., Berthier E., Bhambri R., Brown I., Burgess D.O., Burgess E.W., Cawkwell F., Chinn T., Copland L., Cullen N.J., Davies B., De Angelis H., Fountain A.G., Frey H., Giffen B.A., Glasser N.F., Gurney S.D., Hagg W., Hall D.K., Haritashya U.K., Hartmann G., Herreid S., Howat I., Jiskoot H., Khromova T.E., Klein A., Kohler J., König M., Kriegel D., Kutuzov S., Lavrentiev I., Le Bris R., Li X., Manley W.F., Mayer C., Menounos B., Mercer A., Mool P., Negrete A., Nosenko G., Nuth C., Osmonov A., Pettersson R., Racoviteanu A., Ranzi R., Sarikaya M.A., Schneider C., Sigurdsson O., Sirguey P., Stokes C.R., Wheate R., Wolken G.J., Wu L.Z. & Wyatt F.R. 2014. The Randolph Glacier Inventory: a globally complete inventory of glaciers. *Journal of Glaciology 60*, 537–552, doi: 10.3189/2014JoG13J176.

Porter C., Morin P., Howat I., Noh M.-J., Bates B., Peterman K., Keesey S., Schlenk M., Gardiner J., Tomko K., Willis M., Kelleher C., Cloutier M., Husby E., Foga S., Nakamura H., Platson M., Wethington Jr. M., Williamson C., Bauer G., Enos J., Arnold G., Kramer W., Becker P., Doshi A., D'Souza C., Cummens P., Laurier F., Bojesen M. & Foundation N.S. 2018. ArcticDEM Strips, version 3, doi: 10.7910/DVN/OHHUKH.

Racoviteanu A.E., Paul F., Raup B., Jodha S., Khalsa S. & Armstrong R. 2009. Challenges and recommendations in mapping of glacier parameters from space: results of the 2008 Global Land Ice Measurements from Space (GLIMS) workshop, Boulder, Colorado, USA. *Annals of Glaciology 50*, 53–69, doi: 10.3189/172756410790595804.

Radić V., Bliss A., Beedlow A.C., Hock R., Miles E. & Cogley J.G. 2014. Regional and global projections of twenty-first century glacier mass changes in response to climate scenarios from global climate models. *Climate Dynamics 42*, 37–58, doi: 10.1007/s00382-013-1719-7.

Rastner P., Strozzi T. & Paul F. 2017. Fusion of multi-source satellite data and DEMs to create a new glacier inventory for Novaya Zemlya. *Remote Sensing 9*, article no. 1122, doi: 10.3390/rs9111122.

Raup B., Racoviteanu A., Khalsa S.J.S., Helm C., Armstrong R. & Arnaud Y. 2007. The GLIMS geospatial glacier database: a new tool for studying glacier change. *Global and Planetary Change 56*, 101–110, doi: 10.1016/j.gloplacha.2006.07.018.

Rounce D.R., Hock R., Maussion F., Hugonnet R., Kochtitzky W., Huss M., Berthier E., Brinkerhoff D., Compagno L., Copland L., Farinotti D., Menounos B. & McNabb R.W. 2023. Global glacier change in the 21st century: every increase in temperature matters. *Science 379*, 78–83, doi: 10.1126/science.abo1324.

Screen J.A. & Simmonds I. 2010. The central role of diminishing sea ice in recent Arctic temperature amplification. *Nature 464*, 1334–1337, doi: 10.1038/nature09051.

Sharov A.I. 2005. Studying changes of ice coasts in the European Arctic. *Geo-Marine Letters 25*, 153–166, doi: 10.1007/s00367-004-0197-7.

Smith T.M., Reynolds R.W., Peterson T.C. & Lawrimore J. 2008. Improvements to NOAA's historical merged land–ocean surface temperature analysis (1880–2006). *Journal of Climate 21*, 2283–2296, doi: 10.1175/2007JCLI2100.1.

Sommer C., Seehaus T., Glazovsky A. & Braun M.H. 2022. Brief communication: increased glacier mass loss in the Russian Arctic (2010–2017). *The Cryosphere 16*, 35–42, doi: 10.5194/tc-16-35-2022.

Sun Z., Lee H., Ahn Y., Aierken A., Tseng K.-H., Okeowo M.A. & Shum C.K. 2017. Recent glacier dynamics in the northern Novaya Zemlya observed by multiple geodetic techniques. *IEEE Journal of Selected Topics in Applied Earth Observations and Remote Sensing 10*, 1290–1302, doi: 10.1109/JSTARS.2016.2643568.

Tape K.D., Christie K., Carroll G. & O'Donnell J.A. 2016. Novel wildlife in the Arctic: the influence of changing riparian ecosystems and shrub habitat expansion on snowshoe hares. *Global Change Biology 22*, 208–219, doi: 10.1111/gcb.13058.

Tepes P., Nienow P. & Gourmelen N. 2021. Accelerating ice mass loss across Arctic Russia in response to atmospheric warming, sea ice decline, and Atlantification of the Eurasian Arctic shelf seas. *Journal of Geophysical Research—Earth Surface 126*, e2021JF006068, doi: 10.1029/2021JF006068.

Vaughan D.G., Comiso J.C., Allison I., Carrasco J., Kaser G., Kwok R., Mote P., Murray T., Paul F., Ren J., Rignot E., Solomina O., Steffen K. & Zhang T. 2013. Observations: cryosphere. In T.F. Stocker et al. (eds.): *Climate change 2013: the physical science basis. The Working Group I Contribution to the fifth assessment report of the Intergovernmental Panel on Climate Change*. Pp. 317–382. Cambridge: Cambridge University Press.

Wijngaard J.B., Klein Tank A.M.G. & Können G.P. 2003. Homogeneity of 20th century European daily temperature and precipitation series. *International Journal of Climatology 23*, 679–692, doi: 10.1002/joc.906.

Zeeberg J. 2001. *Climate and glacial history of the Novaya Zemlya Archipelago, Russian Arctic: with notes on the region's history of exploration*. Amsterdam: Rozenberg Publishers.

Zeeberg J. & Forman S.L. 2001. Changes in glacier extent on north Novaya Zemlya in the twentieth century. *The Holocene 11*, 161–175, doi: 10.1191/095968301676173261.

Zhang H.-M., Huang B., Lawrimore J., Menne M. & Smith T.M. 2019. NOAA Global Surface Temperature Dataset, version 5.0, doi: 10.25921/9QTH-2P70. National Ocean and Atmospheric Administration National Centers for Environmental Information. Accessed on the internet at https://www.ncei.noaa.gov/products/land-based-station/noaa-global-temp on 1 October 2023.